Binding of Porphyrins to Tubulin Heterodimers

Fang Tian, Eric M. Johnson, Miguel Zamarripa, Samuel Sansone, and Lorenzo Brancaleon*

Department of Physics and Astronomy, University of Texas at San Antonio, San Antonio, Texas 78249

Received June 21, 2007; Revised Manuscript Received September 28, 2007

We have investigated the binding of two porphyrins, meso-tetrakis (*p*-sulfonatophenyl) porphyrin (TSPP) and protoporphyrin IX (PPIX), to tubulin α,β-heterodimers. TSPP had been shown to directly target microtubules in cells. A comparative study between TSPP and PPIX was carried out because the latter is used in clinical applications and is hydrophobic, in comparison with the water soluble TSPP. The results presented in this manuscript show that both porphyrins bind tubulin with nearly identical stoichiometry but with different affinity (1.76×10^5 M^{-1} for PPIX; 1.1×10^6 M^{-1} for TSPP). The combination of spectroscopic data and molecular simulations suggests that both porphyrins bind as monomers and that their binding site is in proximity of one (or more) Trp residues but do not overlap with the binding site of other well characterized ligands. Molecular simulations also show that the sites that yield the lower energy minima place the porphyrins near the surface of the protein. In the case of TSPP, binding is favored by replacing the ion−dipole interaction of monodispersed TSPP in water with ion–ion interactions provided by two basic residues (His and Lys) at the location of the binding site. Although preliminary, the data show that porphyrin binding could be used to explain some of the effects that photosensitizers may directly produce on protein targets.

Introduction

Tubulin is a 55 kDa globular protein found as a heterodimer of several variants (α, β, γ, etc.).[1] The most common dimer is the α,β heterodimer.[2] Heterodimers polymerize into microtubules (MTs) with a process which in vivo is GTP dependent and reversible.[2–7] MTs are fundamental supramolecular assemblies which participate in various mechanisms including intracellular signaling, mitosis, morphogenesis, etc.[7–10] Because of its multiple functions, tubulin is often a target for various therapies.[6,11–14] Drugs that target microtubules act by either inhibiting/destabilizing or promoting/stabilizing MT polymerization.[14] MT inhibitors include colchicinoids and vinca alkaloids,[5,12,15] whereas MT promoters include taxoids and nucleotides.[12,13,15–17]

The binding of these molecules to tubulin as well as the location of the binding sites has been well characterized and in some cases atomically resolved.[2,18] Taxoids bind a site located in a globular domain of β-tubulin[2,6] whose occupation is related to the stabilization of MT.[2,17] Colchicinoids bind β-tubulin at the α,β-dimer interface,[18] whereas vinca alkaloids bind at the interface between two consecutive α,β-dimers.[18] In addition, α- and β-tubulin present a site for nucleotides that is located at both the inter- and intradimeric interface. In α-tubulin, the site is always occupied by a GTP molecule, while, in β-tubulin, it can be occupied by either GTP or GDP depending on the location along the MT.[3,18]

A decade ago, it was suggested that some types of porphyrins colocalize with MTs, in vivo, and stabilize them with a mechanism reminiscent of the one induced by taxol, thus triggering apoptosis.[10,19] Conversely, other studies indicated a destabilization of microtubules in vitro which was linked to the neurotoxicity of some porphyrins.[20]

Regardless of the macroscopic effect, to this day, there has been no detailed investigation to explain the molecular mechanisms of interaction between tubulin and porphyrins and its biomedical relevance.

In this study, we have considered a simple system of α,β-tubulin dimers interacting with either protoporphyrin IX (PPIX) or meso-tetrakis (*p*-sulfonatophenyl) porphyrin (TSPP).

PPIX is a powerful photoactive drug used in phototherapy of some tumors[21] and in clinical settings is administered as a precursor (5-aminolaevulinic acid, ALA).[22] Its interaction with tubulin has never been investigated.

TSPP has not reached clinical applications but has been shown to affect MTs.[10,19]

Although the apoptotic response induced by porphyrin phototherapy is supposed to be produced by a damage to mitochondria and ER, from the purely biophysical standpoint, the interaction of porphyrins with tubulin is interesting because PPIX is substantially hydrophobic while TSPP is water soluble.

In this study, we have used optical spectroscopies to investigate the interaction between tubulin and porphyrins as a first attempt to explain the mechanisms of interaction and to quantify the affinity of porphyrins for tubulin.

Binding to proteins causes the absorption and fluorescence of porphyrins to change in intensity and shift toward longer wavelength.[23,24] The intrinsic emission of proteins can also be used to investigate the ligand−protein interactions[25–27] through the effects of the binding on the Trp residues which in tubulin are abundant (four in α and four in β (PDB 1TUB)).

We believe that understanding the molecular and structural mechanisms for the formation of tubulin/porphyrin complexes may (i) advance the way in which phototherapy can be administered and (ii) improve our understanding of the porphyrin neurotoxicity at the molecular level.

Experimental Section

Chemicals. TSPP (Frontier Scientific, UT), PPIX sodium salts (Sigma-Aldrich, St Louis, MO), and microtubule-competent, >99%

* To whom correspondence should be addressed. Address: Department of Physics and Astronomy, University of Texas at San Antonio, One UTSA Circle, San Antonio, TX 78249. Phone: (210) 458 5694. Fax: (210) 458 5191. E-mail: lorenzo.brancaleon@utsa.edu.

10.1021/bm700687x CCC: $37.00
Published on Web 11/19/2007

pure, α,β-tubulin (TL238, Cytoskeleton, Denver, CO) were used without further purification. Paclitaxel (Taxol) was purchased from LC Laboratories (Woburn, MA). Spectroscopic grade dimethyl sulfoxide (DMSO) was also purchased from Sigma-Aldrich and used without further purification.

Buffers. Aqueous phosphate buffers were prepared using deionized water. One tablet of phosphate buffered saline (Sigma-Aldrich) was diluted in 200 mL of water to produce a 10 mM buffer at pH 7.4 (as directed by the manufacturer).

Sample Preparation. *PPIX Fluorescence.* The fluorescence of PPIX was recorded with excitation at 405 nm and emission in the 550–750 nm range. Since PPIX does not dissolve in aqueous solutions, an arbitrary amount of solid porphyrin was first added to a small volume of DMSO. The concentration of this stock was adjusted to 1 mM using absorption spectroscopy of a diluted solution, assuming $\varepsilon_{405nm}^{PPIX} = 2.42 \times 10^5\ M^{-1}\ cm^{-1}$.[28] The 1 mM solution of PPIX in DMSO was then diluted into 1.5 mL of buffer to yield a final concentration of 6.6 ± 0.5 μM with less than 1% DMSO and an optical density for PPIX ∼ 0.15 at 405 nm.

The stock solution of tubulin (10 μM) was prepared by dissolving it directly in buffer. The concentration was assessed using $\varepsilon_{280nm}^{tubulin} = 1.15 \times 10^5\ M^{-1}\ cm^{-1}$.[29] Increasing aliquots (from 10 to 100 μL) of the protein solution were added directly into a 1 cm × 1 cm quartz cell containing 1.5 mL of the aqueous solution of PPIX. The absorption and fluorescence spectra of PPIX were recorded after each addition of the protein. Since the addition of the protein stock into the solution produces a dilution of PPIX, control experiments were carried out by adding the same aliquots of buffer (without tubulin) to an aqueous solution of PPIX at the same (6.6 μM) concentration.

TSPP Fluorescence. The fluorescence of TSPP was recorded with excitation at the point closest to being isosbestic (415 nm) and emission in the 550–750 nm range. TSPP was directly dissolved in buffer to a final concentration of 0.7 ± 0.03 μM where the optical density of TSPP at 415 nm was ∼0.15. The concentration was determined optically using $\varepsilon_{413nm}^{TSPP} = 5.10 \times 10^5\ M^{-1}\ cm^{-1}$.[30] The addition of tubulin, the acquisition of the emission spectra, and the normalization procedure were done as described for PPIX.

Tubulin Fluorescence Quenching. A 1.3 ± 0.2 μM solution of tubulin was prepared fresh for each experiment. At this concentration, the optical density is 0.15 at 280 nm. This excitation wavelength was chosen to maintain consistency with the fluorescence lifetime data where the pulsed source is at 280 nm (see below). However, fluorescence spectra recorded with excitation at 280 nm were compared with those recorded with 295 nm excitation which selectively excites Trp residues. After normalization for the different optical densities, the intrinsic fluorescence of the protein was identical for the two excitation wavelengths.

A stock solution of PPIX in buffer was prepared from the 1 mM solution of PPIX in DMSO. The stock of TSPP was prepared directly in buffer. The final concentration of both porphyrins in the stock was 20 μM. An aliquot of 1.5 mL of the tubulin solution was transferred to a 1 cm × 1 cm quartz cell. Increasing small aliquots (10–100 μL) of the 20 μM solution containing the porphyrin were added to the 1.5 mL aqueous solution of tubulin, and the fluorescence of the protein was recorded after each addition. The intrinsic fluorescence of the protein was recorded between 299 and 450 nm. Since the addition of the porphyrin produces a dilution of the protein, control experiments were carried out by adding the same volume of buffer without porphyrin to a second 1.5 mL solution containing the same concentration of tubulin and recording the fluorescence of the protein after each addition.

Quenching of N-acetyl-L-tryptophanamide (NATA) Fluorescence. The porphyrin-induced quenching of NATA fluorescence was carried out as a model for Trp quenching in tubulin.[26] Fluorescence quenching of NATA induced by the addition of PPIX or TSPP was carried out as described previously for tubulin. The concentration of NATA was kept equal to the concentration of tubulin (1.3 ± 0.2 μM). NATA emission spectra were recorded with excitation at 280 and 295 nm. Quenching was analyzed using the Stern−Volmer equation.

Fluorescence Lifetime. Tubulin. The fluorescence lifetime of tubulin was recorded as a function of porphyrin concentration. Measurements were carried out on the same samples used for steady-state fluorescence quenching. Fluorescence decay was recorded with excitation at 280 nm and emission at 330 ± 4 nm, using the shortest window (58 ns) allowed by our instrument which corresponds to a temporal resolution of 56.6 ps/channel.

Porphyrin Lifetime. Fluorescence lifetime was measured upon excitation at 405 nm. Porphyrin lifetimes were recorded (i) before the addition of tubulin and (ii) at a 1:1 tubulin/porphyrin molar ratio where the solution contains almost exclusively tubulin/porphyrin complexes. The fluorescence decay was recorded with emission wavelengths at 620 ± 4 and 631 ± 4 nm for free and bound PPIX, respectively. For TSPP, the wavelengths were 642 ± 4 and 649 ± 4 nm for free and bound porphyrin, respectively. Acquisitions were collected at the same temporal resolution of the tubulin measurements.

Fluorescence Resonance Energy Transfer (FRET). Experiments were carried out to establish the occurrence of FRET between Trp residues and bound porphyrins and in so doing estimate the location of the binding sites. Experiments were carried out at a 1:1 tubulin/porphyrin molar ratio.

Polymerization (Turbidity Assay). Polymerization was recorded using the turbidity assay[31,32] which measures the increase in optical density, due to scattering, at a wavelength (340 nm) where the protein and the porphyrins do not substantially absorb. These experiments were carried out using a fixed concentration of 5 μM tubulin in buffer. This concentration is 5 times larger than the one used for the fluorescence experiments; however, this is necessary in order to record scattering signals with good S/N ratio at 340 nm. Scattering was measured using the dual beam UV–vis spectrophotometer. Polymerization studies were carried out in samples containing tubulin alone, tubulin in the presence of a fixed amount of porphyrins, and upon addition of taxol. On the basis of published results,[31] the concentration of TSPP and PPIX was set at 2.5 μM (2:1 tubulin/porphyrin ratio).

Molecular Docking. Molecular simulations of the docking of TSPP and PPIX to tubulin were carried out using the software Arguslab 4.0.1 (Planaria Software LLC, Seattle, WA). TSPP and PPIX molecules were built using ChemSketch (Advanced Chemistry Development Inc., Toronto, ON, Canada) and optimized using Arguslab. Tubulin α,β-dimer was downloaded from the Protein Data Bank (file PDB 1TUB). The docking was done by approaching the ligand to different sites of the dimer, as well as the intradimeric space, and running calculations using the AScore algorithm of the software.

Instrumentation. Absorption spectra were recorded with a dual beam Evolution 300 spectrophotometer (ThermoElectron, Madsion, WI). Spectra were recorded with 2 nm resolution and 240 nm/min speed. Porphyrin spectra were recorded between 250 and 700 nm, while tubulin absorption spectra were recorded between 220 and 450 nm. Appropriate baseline and reference cells were used for each scan.

Fluorescence spectra were recorded using a double-monochromator AB2 fluorimeter (ThermoElectron, Madison, WI) setting a 4 nm bandpass in excitation and emission and acquisition speed at 2 nm/s.

Fluorescence lifetime was recorded using a time-correlated single photon counting (TCSPC) instrument (IBH 5000U, Horiba Jobin Yvon, Edison, NJ). Porphyrin fluorescence decay was recorded upon excitation with a pulsed diode laser at 405 nm (Nano-LED-07, pulse width ∼ 150 ps), while tubulin fluorescence decay was recorded upon excitation with a pulsed LED source at 280 nm (Nano-LED-15, pulse width ≈ 750 ps). Both sources are manufactured by IBH Ltd. (Glasgow, U.K.) and are operated at a repetition rate of 1 MHz. The instrument response function (IRF), prompt, was recorded after or before each decay curve using suspensions of glycogen (0.1 mg/mL) in deionized water. All signals were recorded at a counting rate between 2000 and 12 000 cts/s which is well below the suggested maximum counting rate (20 000 cts/s) corresponding to 2% of the source's repetition rate.

Data Analysis

Because of the complexity of the system and the limitation of the individual methods described below, the binding parameters (binding constant, number of sites, etc.) were calculated using a combination of porphyrin fluorescence and tubulin quenching.

Porphyrin Fluorescence. Changes of porphyrin fluorescence upon binding (Figure 1) can be analyzed with different methods which depend on the experimental procedure used. All methods assume that the following reaction takes place:

$$n[\text{porphyrin}]_f + [\text{tubulin}] \rightleftarrows [\text{porphyrin}]_b \quad (1)$$

where $[\text{porphyrin}]_f$ and $[\text{porphyrin}]_b$ are the concentration of free and bound ligand and n is the number of porphyrin molecules bound to each protein molecule. Assuming n noninteracting sites and one ligand per site

$$K_b = \frac{[\text{porphyrin}]_b}{n[\text{tubulin}]_f[\text{porphyrin}]_f} \quad (2)$$

where K_b represents the binding constant in M^{-1}. In our case, the free and bound porphyrins are determined using fluorescence spectroscopy (see below). Most methods used in the past to exploit the overall fluorescence of the ligand were designed for ligands whose emission intensity is negligible in the free form (e.g., 1-anilinonaphthalene-8-sulfonic acid (1,8-ANS)) so that the fluorescence recorded can be entirely assigned to the bound molecule.[32,33] With porphyrins, however, the contribution of the free molecule cannot be neglected. Thus, in order to separate the contribution of free and bound porphyrin, the emission spectrum was analyzed using Gaussian spectral fitting.

Gaussian Spectral Fitting. The contributions of free and bound porphyrins were calculated by fitting each emission spectrum with Gaussian components. The rationale is relatively straightforward. The emission spectra of a mixture of free and bound porphyrin is a linear combination of the spectra of the individual components

$$I(\lambda) = [L]_f I_f(\lambda) + [L]_b I_b(\lambda) \quad (3)$$

where $I_f(\lambda)$ and $I_b(\lambda)$ are the emission spectra of the free and bound porphyrin, respectively, while $[L]_f$ and $[L]_b$ are the concentrations of free and bound porphyrin. Typical porphyrin emission spectra (bound or free) contain two peaks (Figure 2), a narrower, more intense one at shorter wavelengths (~600–650 nm) as well as a broader, less intense one at longer wavelengths (~670–750 nm).[23,30,34] Thus, after normalization for absorption, each $I_j(\lambda)$ of eq 3 can be approximated to a linear combination of Gaussians

$$I(\lambda) = [L]_f C \sum_j \Phi_{f,j} G_{f,j}(\lambda) + [L]_b \alpha \sum_j \Phi_{b,j} G_{b,j}(\lambda) \quad (4)$$

where C is an instrumental constant, Φ_j is the fluorescence quantum yield, and $G_j(\lambda)$ is the Gaussian of the jth component to the spectrum centered at wavelength Λ_j.

To simplify the terms in eq 4, we assumed that the binding information is confined to the peak at shorter wavelengths. Thus, if one assumes that this peak is the linear combination of only one $G_{f,j}(\lambda)$ and one $G_{b,j}(\lambda)$, eq 4 can be written as

$$I(\lambda) = A_f e^{-(\lambda - \Lambda_f)^2/\Delta_f} + A_b e^{-(\lambda - \Lambda_b)^2/\Delta_b} + \sum_j A_j e^{-(\lambda - \Lambda_j)^2/\Delta_j} \quad (5)$$

where Λ_f and Λ_b are the peak positions of the free and bound Gaussian, respectively, for the first peak (Figure 2). The value of Λ_f is 621 ± 1 nm for PPIX and 642 ± 1 nm for TSPP, whereas the value of Λ_b is 631 ± 1 nm for PPIX and 649 ± 1 nm for TSPP. The amplitudes (A) contain both the concentration of each

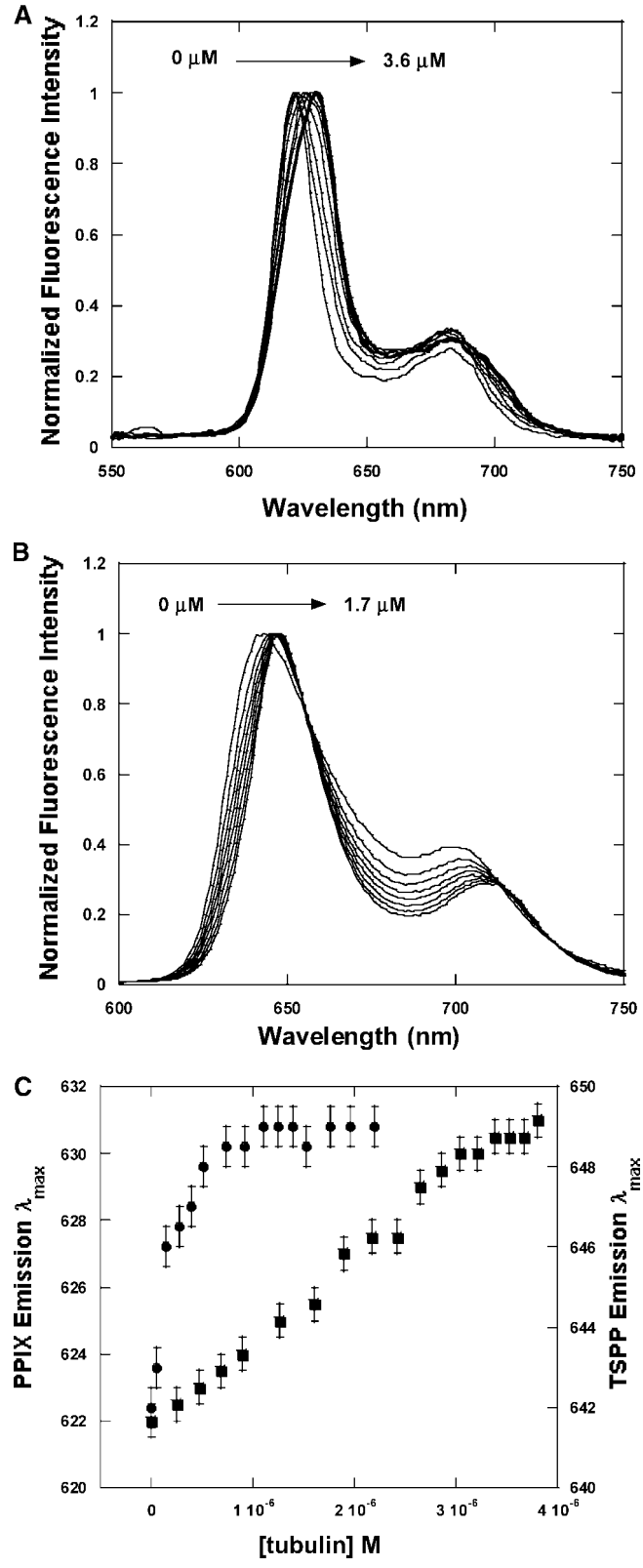

Figure 1. (A) Emission spectra of PPIX as a function of the concentration of tubulin (0–3.6 μM). (B) Emission spectra of TSPP as a function of the concentration of tubulin (0–1.7 μM). In both figures, the arrow highlights the red-shift of the first emission maximum caused by the addition of tubulin. (C) Position of the first emission maximum of PPIX (■) and TSPP (●) as a function of tubulin concentration. Please note that the scale of the *y*-axis is different for the two porphyrins.

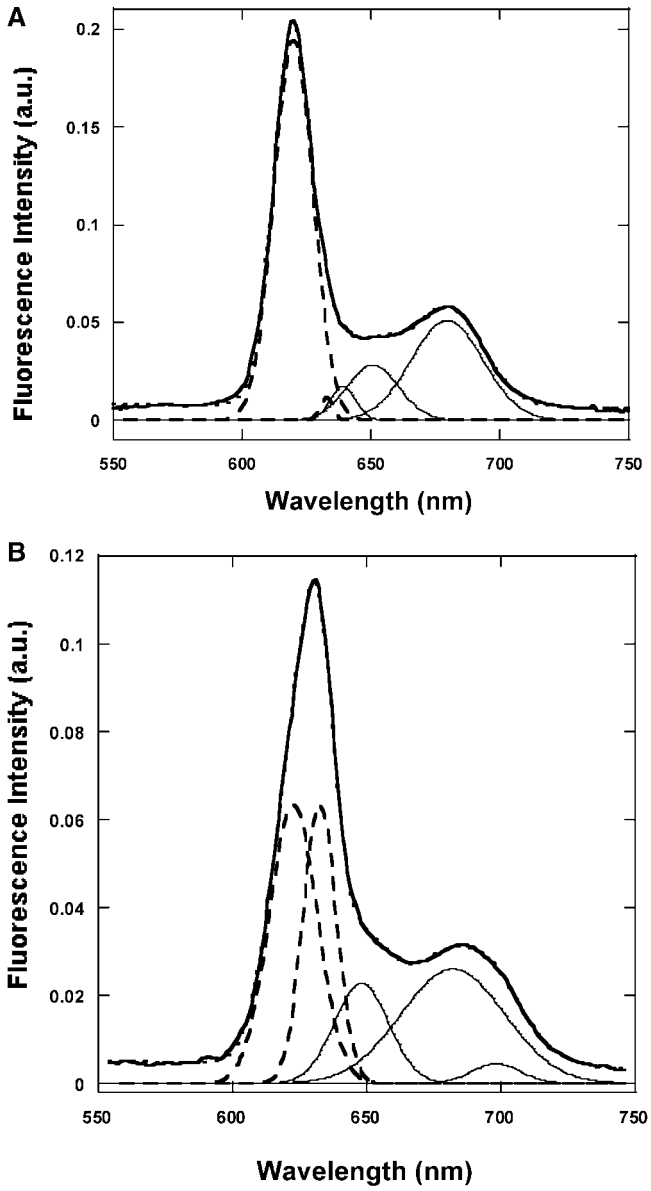

Figure 2. (A) Fitting of the emission spectrum of PPIX + 0.47 μM tubulin using five Gaussian components: (—) experimental spectrum; (- - -) fitted curve using eq 5; (— — —) Gaussian components corresponding to free and bound PPIX (eq 5); (—) additional Gaussian components according to the last summation of eq 5. The fitted curve is not easy to see because it is overlapped with the experimental spectrum. (B) Same as in part A but at a 2.4 μM tubulin concentration.

species and the quantum yield associated with it.

The last summation of eq 5 fits the "rest" of the spectrum, i.e., the region of the second peak. This region is less sensitive to the effects of porphyrin binding and is produced by an unknown number of components. Thus, we assumed this portion of the spectrum as having the same number of components for free and bound porphyrin. This enabled us to fit the emission spectra with a minimum number of Gaussian components, as the last term of eq 5 required the introduction of only two to three additional components.

Each Gaussian carries three free parameters: amplitude (A_j), peak wavelength (Λ_j), and width (Δ_s). During the fitting procedure, the values of Λ_f and Λ_b were constrained to vary within 2 nm of the experimentally determined peak positions. The value of Λ_f was assumed to be the one obtained from the spectrum recorded in the absence of tubulin. Conversely, Λ_b was assumed to be the one retrieved from the most red-shifted position of the emission maximum induced by addition of tubulin, since the position of the emission peak reaches a plateau (Figure 1C).

The quality of fitting was determined by visual inspection and using the value of χ^2 as a reference. Since the amplitude of each Gaussian contains the Φ_j value and the concentration of the emitting species, the areas obtained through the fitting do not directly yield the concentration of free and bound porphyrin; rather, they provide the products $\Phi_f[L]_f$ and $\Phi_b[L]_b$. These values can be used to determine the binding parameters as shown below.

Use of Gaussian Fitting to Determine the Binding Parameters. From eq 2, for n independent binding sites the following equation can be written:[35]

$$\frac{[\text{porphyrin}]_b}{[\text{tubulin}]} = \frac{nK_b[\text{porphyrin}]}{1 + K_b[\text{porphyrin}]} \tag{6}$$

where [porphyrin] is the total concentration of the ligand. Considering that the Gaussian fitting provides the values of $\Phi_f[L]_f$ and $\Phi_b[L]_b$ (Figure 2), eq 6 can be modified as

$$\frac{[\text{porphyrin}]_b}{[\text{tubulin}]} = \frac{\frac{nK_b}{\Phi_b}[\text{porphyrin}]}{1 + K_b[\text{porphyrin}]} \tag{7}$$

The fitting with eq 7 yields K_b and the ratio n/Φ_b.

The same set of data obtained from Gaussian fitting can also be used using the method suggested by Davila and Harriman[36] who developed the following equation for analyzing the fluorescence of a zinc porphyrin to albumin

$$\log\left(\frac{\Phi_b\delta}{n - \Phi_b\delta}\right) = a \log[\text{porphyrin}]_f - a \log K_d \tag{8}$$

where δ is the ratio between the concentration of bound porphyrin and the concentration of tubulin. This provides an independent method to calculate n and K_b.

Tubulin Fluorescence Quenching. Fluorescence quenching does not introduce the uncertainties that the fluorescence of the ligand produces. Static quenching, due to binding, is exclusively related to the number of fluorophores that are quenched.[37] Therefore, quenching of tubulin intrinsic fluorescence can be used to retrieve several binding parameters.

The raw fluorescence data, calculated as the area of the emission spectrum in the 300–450 nm range, were corrected for the slight contribution of the porphyrin absorption according to the equation[38,39]

$$F_{corr} = 10^{A_{ex}+A_{em}/2}F_{raw} \tag{9}$$

where A_{ex} and A_{em} are the optical density at the excitation (280 nm) and emission wavelength maximum (333 nm) of tubulin while F_{raw} is the raw area of the emission of the protein.

F_{corr} was further corrected for the fact that binding of porphyrin molecules to tubulin only produces partial quenching of the protein fluorescence. This problem had been recognized in the past by Lehrer who proposed a method to calculate the fractional quenching for collisional mechanisms.[40] Stern−Volmer and other methods of analysis of fluorescence quenching assume that the ligand/protein complex is nonfluorescent. In the presence of multiple Trp residues, this assumption may not be valid. Tubulin dimers have eight Trp residues, and it is unlikely that they are all quenched by the binding of porphyrin molecules.

If one assumes that $\Phi_F[\text{tubulin}]_0$ is the fluorescence of the unquenched tubulin, while $\Phi_F[\text{tubulin}]_0 - [\text{porphyrin}]$ is the fluorescence of the mixture after addition of the quencher (with Φ_F being the fluorescence quantum yield of the protein), the fractional fluorescence decrease can be represented by the equation[41]

$$\frac{I}{I_0} = 1 - \alpha\frac{[\text{porphyrin}]}{[\text{tubulin}]} \tag{10}$$

where α is the fraction of protein fluorescence quenched by the binding of a porphyrin molecule and can be retrieved via the linear regression of eq 10. This correction is important because, for instance, if only a portion of the protein is quenched, the slope of the Stern−Volmer plot would underestimate the binding constant. This second correction yields

$$F_\alpha = (1 - \alpha)F_{\text{corr}} \tag{11}$$

which is the value used in our data analysis.

After correction of the protein emission, quenching data were analyzed using several methods.

Stern−Volmer. In spite of the two exposed Trp residues (Trp 346α and Trp 407β), the fluorescence decay of the protein does not change with the addition of porphyrins (see the Results section); thus, we assume that the fluorescence quenching is dominated by static interaction. Classic theory of static quenching predicts that the relative decrease of the fluorescence is described by

$$\frac{F_0}{F_\alpha} = e^{VN_A[Q]} \tag{12}$$

where F_0 is the starting, corrected, fluorescence intensity in the absence of quencher and F_α is the fluorescence intensity in the presence of quencher [Q] corrected through eq 10. The product VN_A has the units of a binding constant, K_b (M^{-1}). Equation 12 predicts an upward-curved plot of F_0/F versus [Q] and applies also when the concentration of bound quencher is comparable to the concentration of the total quencher.[42]

At low quencher concentration, eq 12 reduces to[39]

$$\frac{F_0}{F_\alpha} = 1 + K_b[Q] \tag{13}$$

The Stern−Volmer plot of eq 13 yields the estimate of K_b as observed by fluorescence quenching. This value can be compared to the one obtained using the porphyrin fluorescence (eq 7) to test similarities or discrepancies of two independent measurements.

Double Logarithmic Plot. Assuming that only one porphyrin molecule binds to each binding site, the following equation can be obtained[43–45]

$$\left(\frac{F_0 - F_\alpha}{F_\alpha - F_\infty}\right) = \left(\frac{[\text{porphyrin}]}{K_d}\right)^n \tag{14}$$

where K_d is the dissociation constant ($1/K_b$) and F_∞ is the extrapolated residual fluorescence at infinite concentration of quencher (calculated as the intercept of $1/(F_0 - F_\alpha)$ vs 1/[porphyrin]). The plot of log $[(F_0 - F_\alpha)/(F_\alpha - F_\infty)]$ versus log[porphyrin] yields the number of binding sites the value of K_b (i.e., $1/K_d$) from the intercept at log $[(F_0 - F_\alpha)/(F_\alpha - F_\infty)] = 0$. These values are therefore calculated independently from those obtained from the porphyrin fluorescence.

Fluorescence Resonance Energy Transfer (FRET). This technique probes the transfer of energy from the excited state of a donor to the ground state of an acceptor and can be used to estimate the distance between two molecules according to the equation[46]

$$E = \frac{R_0^6}{R_0^6 + R^6} \tag{15}$$

where R is the estimated distance between donor and acceptor while R_0 is the distance corresponding to a transfer efficiency of 50%. The efficiency of FRET (E) is calculated as

$$E = 1 - \frac{I}{I_0} = 1 - \frac{\tau}{\tau_0} \tag{16}$$

where I and τ are the fluorescence intensity and fluorescence lifetime of the donor in the presence of the acceptor while I_0 and τ_0 are the intensity and fluorescence lifetime of the donor in the absence of the acceptor. R_0 depends on the overlap integral (J) between the donor's emission spectrum and the acceptor's absorption spectrum, the geometric factor (k), the quantum yield of the donor (φ_D), and the average refractive index of the medium.[46] In this case, the Trp residue in tubulin is the donor and the porphyrin molecule noncovalently bound to the protein is the acceptor.

When studying FRET, one has to be aware that, although the donor fluorescence is quenched in the process, the quenching of the donor does not automatically imply the occurrence of FRET. Quenching can occur by other mechanisms when the distance (d) between donor and acceptor is much smaller than R_0 or this is small enough that it requires the donor and acceptor to be in such close proximity that direct perturbation of the excited state of the donor results in nonradiative decay without transfer.[46] Thus, the occurrence of FRET must be investigated with a combination of fluorescence measurements including emission spectroscopy, excitation spectroscopy, and fluorescence decay.

Emission spectroscopy investigated whether porphyrin (acceptor) fluorescence was produced upon excitation of the Trp residues (donor). Vice versa, excitation spectroscopy investigated whether the Trp excitation spectrum is produced upon setting the emission wavelength at the fluorescence maximum of the poprhyrin. Control experiments were carried out in solutions containing tubulin alone and porphyrin alone in order to rule out (or in) artifacts due to the protein itself.

FRET was also estimated by recording the emission decay of the donor with and without the bound acceptor (eq 16).

Turbidy Assay. This method has been used extensively in the past to observe the aggregation of tubulin in solution.[31] With this assay, the apparent relative optical density is recorded at 340 nm. At this wavelength, there is no contribution from Trp absorption; thus, changes of apparent optical density can be entirely attributed to changes in the scattering property of the solution which increases with the aggregation of the protein. Apparent absorption at 340 nm was recorded as a function of time for up to 3 h. These experiments were used to determine whether binding of porphyrins induced a polymerization of the α,β-tubulin dimers. All experiments were carried out at room temperature, 22 ± 2 °C. Since the solution used does not contain either glycerol or Mg^{2+}, tubulin was not expected to aggregate into MT spontaneously.[47]

Molecular Docking. Docking of TSPP and PPIX to tubulin was carried out using Arguslab 4.0.1 (Planaria Software LLC, Seattle, WA). TSPP and PPIX molecular models were created using Chemsketch (ACD/Laboratories, Toronto, ON, Canada) and their molecular structure optimized using the PM3 semiempirical QM method available with Arguslab. The tubulin

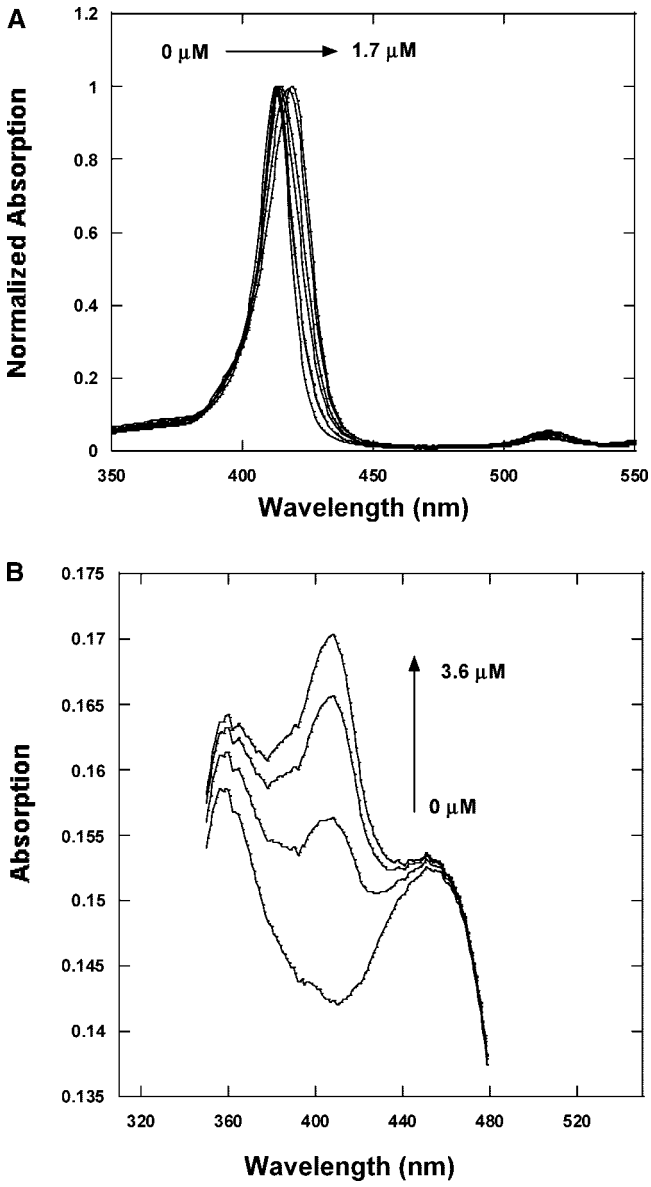

Figure 3. (A) Absorption spectra of TSPP upon addition of tubulin. The arrow indicates the red-shift of absorption from 413 to 420 nm. Notice the absence of absorption bands near 490 nm normally associated with the formation of aggregates. (B) Absorption spectra of PPIX upon addition of tubulin. The peak of monomeric (bound) PPIX appears and increases (arrow) over the broad, poorly structured spectrum of PPIX in buffer.

structure used to dock the porphyrins was 1TUB from the Protein Data Bank and was directly imported into Arguslab. For the docking, each porphyrin was placed in the region of a possible binding site, and after the software created the binding site, docking was carried out by minimizing the interaction energy between the ligand and the site using the AScore algorithm. Several sites were probed including the taxol, nucleotide, and colchicine sites (as determined from PDB 1TUB, Protein Data Bank files). Other sites in proximity of each Trp residue were also probed.

Results

Absorption Spectroscopy of Binding Porphyrins. The addition of increasing aliquots of tubulin to the aqueous solution produced a red-shift of the absorption maximum of TSPP (Figure 3A) and the appearance of a peak at 405 nm over the

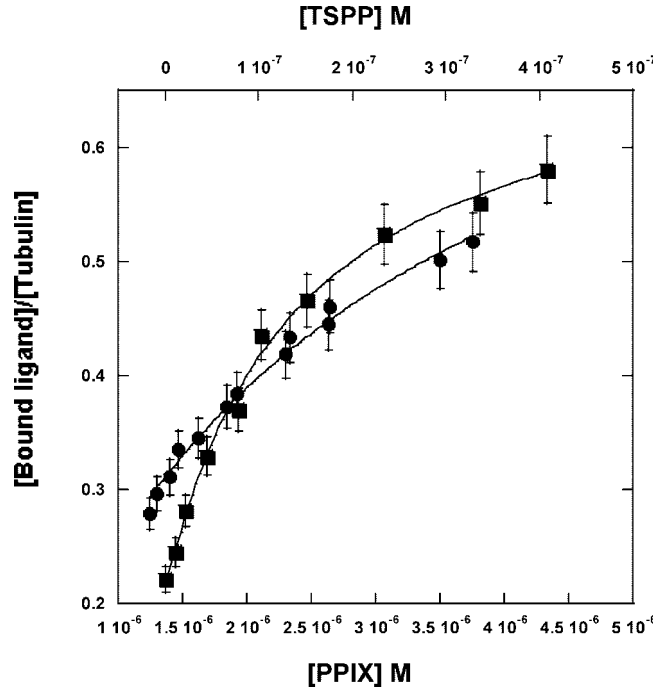

Figure 4. Binding curves obtained from Gaussian fitting (eq 7): (●) PPIX; (■) TSPP. Note that the scale of the *x*-axis is different for the two porphyrins.

unstructured spectrum of PPIX (Figure 3B). This is in agreement with what was observed in other studies of porphyrin/protein noncovalent binding and has been explained as (i) binding of porphyrin macrocycles to nonaqueous sites[28,48] and/or (ii) monodispersion.[24,49] Figure 3A also shows that binding of TSPP to tubulin does not induce formation of J-aggregates, as observed in other studies.[30]

Porphyrin Fluorescence. Addition of tubulin to the solution causes the emission of TSPP or PPIX to increase in intensity and shift to longer wavelengths (Figure 1). The maximum of TSPP shifts from 642 to 649 nm, and the maximum of PPIX shifts from 620 to 631 nm (Figure 1C). The Gaussian fitting of the emission spectra (Figure 2) shows that, as more tubulin is added to solutions containing porphyrin, the peak of bound porphyrin increases relatively to the one of free porphyrin. The areas of the Gaussians associated with bound and free porphyrin yield the value of $\Phi_b[L]_b$ and $\Phi_f[L]_f$, respectively.

Upon substitutions of the values and fitting with eq 7 (Figure 4), we retrieved values of $K_b = 2.19\ (\pm 0.64) \times 10^5\ M^{-1}$ and $K_b = 2.22\ (\pm 0.29) \times 10^6\ M^{-1}$ for PPIX and TSPP, respectively. From the values of K_b, the ratio n/Φ_b was calculated as 9.8 ($\pm$2.1) for PPIX and 3.8 ($\pm$0.9) for TSPP.

By fitting the data with eq 8, one can then independently obtain an estimate for n and Φ. The analysis with eq 8 yields $n = 1.3 \pm 0.5$ and $n = 1.2 \pm 0.4$ for PPIX and TSPP, respectively. From the values of n, Φ_b was estimated at 0.13 for PPIX and 0.26 for TSPP.

Quenching of Tubulin Fluorescence. Addition of TSPP or PPIX to tubulin solutions quenches the intrinsic fluorescence of the protein. The effect is accompanied by a slight blue-shift of the protein emission maximum which is smaller for PPIX ($\Delta\lambda = 2$ nm) than for TSPP ($\Delta\lambda = 4$ nm) (Figure 5).

Because of the presence of multiple Trp residues in tubulin, fluorescence analysis requires that we determine the fraction of tubulin fluorescence that is quenched by porphyrin.

Fractional Fluorescence Change. The fraction of quenched tubulin fluorescence can be estimated using eq 10. The linear

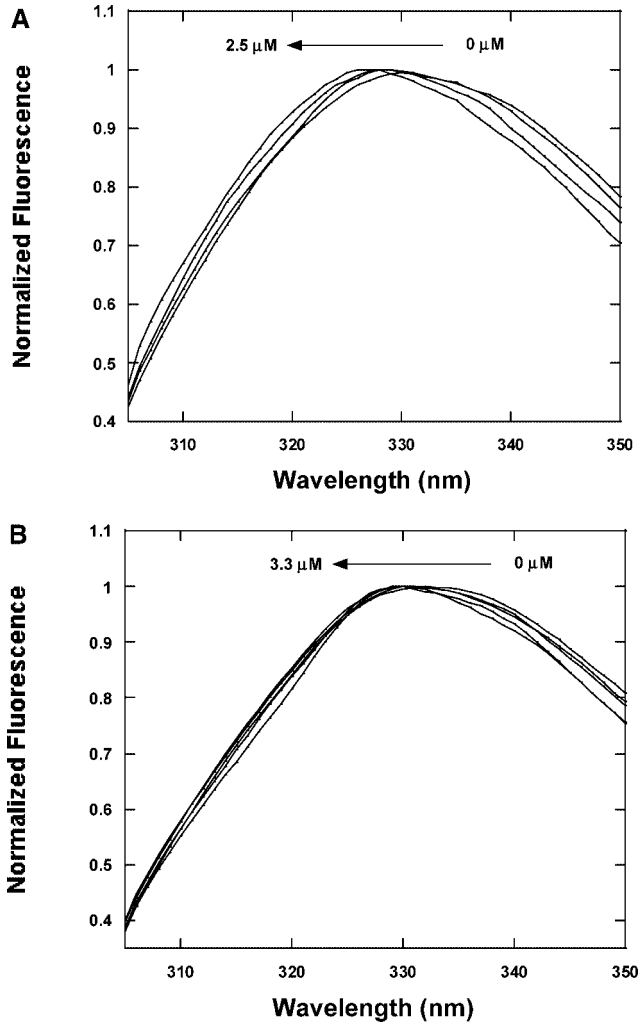

Figure 5. Effects of porphyrin on tubulin fluorescence. Addition of TSPP (A) and PPIX (B) produces a shift to shorter wavelength (arrow) of the emission maximum of tubulin.

regression yielded values of $\alpha = 0.10 \pm 0.02$ and $\alpha = 0.14 \pm 0.08$ for PPIX and TSPP, respectively. The values are similar to the ones that were obtained using the crude extrapolation of the reciprocal plot ($F_0/\Delta F$ vs 1/[Q]) proposed by Lehrer for collisional quenching ($\alpha = 0.11 \pm 0.02$ and $\alpha = 0.25 \pm 0.11$).

The value of α was then used in the analysis with eqs 13 and 14.

Stern−Volmer. The S−V plots show an upward curvature for quenching with either porphyrin (Figure 6). This may suggest the overlap of a dynamic and a static quenching component which could be justified by the presence of two exposed Trp residues (Trp 346α and Trp 407β). However, since the fluorescence lifetime of tubulin does not change under these conditions (see below), a dynamic component to the quenching was ruled out. Therefore, we assumed that the quenching was purely static (eq 12) and at low porphyrin concentration could be described by eq 13 (inset of Figure 6). The linear limit was different for PPIX (<3 μM) and TSPP (<1 μM), and the linear regression yielded $K_b = 1.41\ (\pm 0.29) \times 10^5\ M^{-1}$ for PPIX and $K_b = 7.20\ (\pm 0.47) \times 10^5\ M^{-1}$ for TSPP.

Double Logarithmic Plot. The plot of log $[(F_0 - F_\alpha)/(F_\alpha - F_\infty)]$ versus log[porphyrin] (eq 14) is linear (Figure 7). The slope of the linear regression yields the number of independent binding sites $n = 1.1 \pm 0.10$ for PPIX and $n = 0.8 \pm 0.04$ for TSPP. The value of log[porphyrin] at log $[(F_0 - F_\alpha)/(F_\alpha - F_\infty)] = 0$ yields $\log(K_d)$[45,50] from which K_b was calculated as 1.67 (±0.62) $\times 10^5$ and 3.11 (±0.41) $\times 10^5$ for PPIX and TSPP, respectively. The value of n is in agreement with the one obtained using porphyrin fluorescence (eq 8), while the value of K_b is smaller. The parameters calculated with different methods are summarized in Table 1.

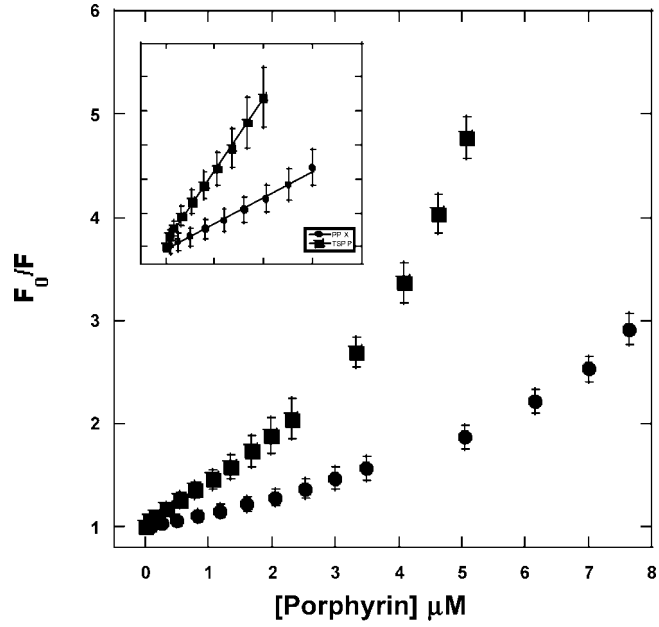

Figure 6. Stern−Volmer plots of tubulin quenching. The main figure shows the deviation from linearity due to static quenching. The inset shows the fitting of the linear portion using eq 13: (●) PPIX; (■) TSPP.

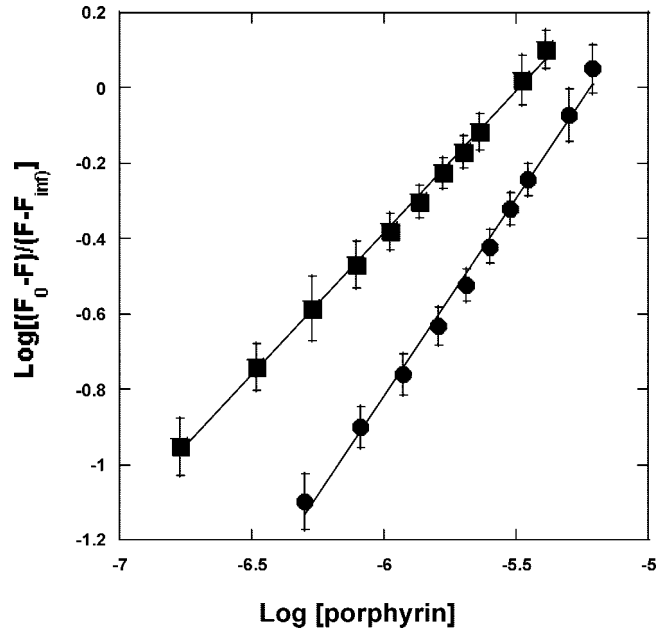

Figure 7. Double logarithmic plot (eq 14) of tubulin quenching induced by PPIX (●) and TSPP (■).

Fluorescence Quenching of NATA. The quenching parameters discussed above are obtained under the hypothesis that the decrease of protein fluorescence is due to the location of a porphyrin near, at least, one Trp residue. However, not all ligands have the same quenching efficiency,[37] and in principle, even if PPIX and TSPP localized at the same distance from the same Trp residue, they may still produce different quenching. In order to investigate these differences, we studied the PPIX CDV

Table 1. Summary of Binding Parameters Obtained from Porphyrin Fluorescence and Tubulin Quenching

parameter	PPIX	TSPP	method
K_b (M^{-1})	2.19 ($\pm$0.64) $\times$ 10^5	2.22 ($\pm$0.29) $\times$ 10^6	eq 7
	1.41 ($\pm$0.29) $\times$ 10^5	7.20 ($\pm$0.47) $\times$ 10^5	eq 13
	1.67 ($\pm$0.62) $\times$ 10^5	3.11 ($\pm$0.41) $\times$ 10^5	eq 14
n	1.3 $\pm$ 0.5	1.2 $\pm$ 0.4	eq 8
	1.1 $\pm$ 0.10	0.8 $\pm$ 0.04	eq 14
Φ_b	0.13	0.26	eq 7 and 8

and TSPP-induced quenching of NATA fluorescence in solution because NATA is often used as a model for the fluorescence of Trp in proteins. Quenching of NATA is collisional, while quenching of Trp residues in tubulin is static; nonetheless, the quenching data would provide an estimate of substantial differences in the quenching efficiency between PPIX and TSPP.

The S−V plots of NATA quenching are linear over the entire concentration of added porphyrin (0–4.5 μM). The retrieved value of the quenching constant (K_s) was 1.19 ($\pm$0.05) $\times$ 10^5 M^{-1} for PPIX and 1.28 ($\pm$0.12) $\times$ 10^5 M^{-1} for TSPP. Thus, TSPP is only slightly more efficient in the collisional quenching of indole fluorescence.

Time Resolved Fluorescence. *Tubulin.* The decay of tubulin intrinsic fluorescence reveals a nonexponential decay with three components (summarized in Table 2). Because of the large number of Trp residues, a complex multiexponential decay is expected.[51]

The relative contribution of the long-lived component (τ > 5 ns) suggests that the more exposed Trp residues may contribute to the majority of the protein fluorescence;[52–54] however, we did not attempt to separate the contribution of the single Trp residues.

Porphyrins. The fluorescence decay of TSPP and PPIX are affected by the binding to tubulin in agreement with previous observations.[23,30,55] PPIX fluorescence decay, which is biexponential in aqueous solution, becomes virtually monoexponential when the porphyrin binds tubulin (Table 3). The relative amplitude of the short-lived component is quite small for the free ligand (6%); however, upon binding of tubulin, its contribution decreases to $\approx$1%. The lifetime of the dominant component increases by approximately 1 ns upon binding to tubulin.

The fluorescence lifetime of TSPP is monoexponential in aqueous solution and after binding to tubulin. However, the lifetime lengthens from 9.9 to 11.7 ns (Table 3).

Fluorescence Decay of Tubulin in the Presence of Porphyrins. The addition of either porphyrin does not change the individual components or the average lifetime of tubulin fluorescence (Table 2, Figure 8). This supports our assumption that the fluorescence quenching of the protein is due entirely to static quenching caused by binding. It also appears to be in agreement with quenching of only a small portion of the Trp residues in tubulin.

FRET. Table 2 and Figure 8 clearly indicate that addition of porphyrins does not affect the fluorescence decay of tubulin, thus suggesting the absence of FRET between Trp residues and porphyrins. Additional support is provided by steady-state emission and excitation spectroscopy. Excitation of tubulin at 280 nm in the presence of PPIX or TSPP does not produce an increase of the porphyrin emission intensity. Likewise, the excitation spectrum of porphyrin−protein mixtures does not show any increase of tubulin contribution when the emission wavelength was fixed to the value of the bound porphyrin.

In fact, excitation spectra of solutions containing only tubulin and no porphyrin, recorded with the emission wavelength at 631 or 649 nm, show a contribution of the protein. Since the protein fluorescence does not contribute at such long wavelengths, we explain this as an artifact due to the fact that the range of emission wavelengths for the porphyrins (630–650 nm) overlaps with the first harmonic of the emission of the protein (315–325 nm), thus causing the appearance of the tubulin excitation spectrum.

Polymerization of Tubulin. We investigated whether the fluorescence effects observed could be attributed to polymerization of tubulin during the fluorescence experiments. To do so, we carried out scattering experiments (turbidity assay[31,32]) under the same conditions of temperature and buffer used for the fluorescence experiments. As expected, by operating at room temperature and in simple phosphate buffered solution, the polymerization of tubulin was inhibited in the time scale of a typical fluorescence experiment (2–3 h) even at much higher tubulin concentration (5 μM). The addition of TSPP and PPIX did not induce any polymerization (Figure 9). We thus ruled out that our results were affected by binding of porphyrin to polymerized tubulin.

Docking Simulation. Docking of PPIX yielded several possible binding configurations. The one characterized by the lower minimum was partly overlapped with the taxol site (−11.9 kcal/mol); however, this site did not produce proximity to any Trp residue, the closest being Trp21 of the β-monomer located >20 Å away from the center of the porphyrin ring. The configuration that produced the best combination of minimum energy (−11.2 kcal/mol) and proximity to Trp residues is a site partly overlapped with the nucleotide site on the β-monomer. Such a site brings PPIX and Trp407 in close contact (Figure 10A). Other sites in the proximity of Trp residues or near the location of the colchicine binding site produced stable configurations with much smaller energy minima (−4.5 kcal/mol < ΔG < −9.0 kcal/mol). Since fluorescence experiments suggest that there are two porphyrins bound to each tubulin dimer, one of these sites, not shown in Figure 10, could represent the second docking location.

Docking of TSPP yielded fewer possible binding configurations than PPIX, likely because of the four negatively charged SO_3^- groups symmetrically distributed around the ring. The one characterized by the lower minimum (−10.6 kcal/mol) is located between the taxol site and the GTP/GDP site on the β-monomer. This configuration also brings the center of the TSPP ring ~11 Å from the N1 atom of the indole ring of Trp21 (Figure 10B). Also, at this site, one of the SO_3^- groups is located equidistant (~5 Å) from two basic residues: His229 and Lys19 (Figure 10C).

Docking of TSPP to the site of taxol, colchicines, vinblastine, as well as sites in proximity of other Trp residues resulted in either no energy minimization or configuration with shallower minima (−5.0 kcal/mol < ΔG < −6.8 kcal/mol). However, because fluorescence data indicate the binding of a second TSPP molecule, it is likely that one of these sites would also be occupied.

An interesting observation is that in nearly all docking configurations, such as the one shown in Figure 10, the indole ring of the most proximal Trp residues and the ring of the porphyrins were nearly at a 90° angle, thus independently supporting the absence of FRET between Trp residues and porphyrins.[46]

Table 2. Decay Parameters of Tubulin Fluorescence with and without Porphyrin

	α_1	τ_1	α_2	τ_2	α_3	α_1
tubulin	0.11 ± 0.08	0.63 ± 0.28	0.36 ± 0.07	2.41 ± 0.31	0.53 ± 0.08	5.30 ± 0.47
tubulin + PPIX	0.15 ± 0.07	0.54 ± 0.29	0.32 ± 0.10	2.29 ± 0.31	0.53 ± 0.11	5.21 ± 0.68
tubulin + TSPP	0.13 ± 0.08	0.58 ± 0.28	0.39 ± 0.12	2.34 ± 0.31	0.48 ± 0.11	5.26 ± 0.71

Table 3. Fluorescence Lifetime of TSPP and PPIX with Tubulin (Excitation 405 nm)

	α_1	τ_1	α_2	τ_2
TSPP	0.02 ± 0.02	1.60 ± 0.12	0.98 ± 0.04	9.90 ± 0.11
TSPP + tubulin	<0.01	<1 ns	0.98 ± 0.03	11.7 ± 0.18
PPIX	0.06 ± 0.02	1.57 ± 0.33	0.94 ± 0.05	14.3 ± 0.15
PPIX + tubulin	<0.01	<1 ns	0.98 ± 0.05	16.5 ± 0.14

More detailed docking studies are ongoing and may shed further light on the location of the binding sites for PPIX and TSPP and the resulting intermolecular interactions.

Discussion

Turbidity assays (Figure 9) confirm that fluorescence results are not affected by the formation of tubulin aggregates and/or microtubule-like structures. Thus, the basis of the following discussion is that binding occurs exclusively between porphyrin molecules and tubulin heterodimers.

Absorption spectra and fluorescence spectra are in agreement with the binding between the two porphyrins and tubulin. In absorption, the appearance of the Soret band of PPIX and the shift from 413 to 420 nm of the Soret band of TSPP is consistent with binding of porphyrins to macromolecules.[30] Unlike other proteins,[30,56] tubulin does not appear to promote formation of J-, or other, aggregates of TSPP, before or after the binding.

Likewise, the shift in the emission spectra and the relative increase of the fluorescence intensity (Figure 1) are consistent with binding of the porphyrin to the tubulin heterodimers.[24,28] Both absorption and emission spectra suggest monomerization of the bound porphyrin. Monomerization of PPIX is confirmed by the virtually monoexponential decay in the presence of tubulin (Table 3). The data are consistent with breakdown of PPIX aggregates and insertion of the porphyrin in a less solvent exposed environment.[28,48,57] Our docking experiments (Figure 10A and others not shown) suggest a slightly different scenario where, indeed, the PPIX monomer binds to tubulin, but the binding sites leave the porphyrin at or near the surface of the protein. This is in agreement with our previous observations that the fluorescence spectrum of PPIX bound to some proteins shows similarities with the spectrum in organic but polar solvents.[23,24,49] Thus, the porphyrin monomerizes upon binding, but its location is such that the polarity of water still influences PPIX emission properties.

Free TSPP, on the other hand, is already monodispersed at pH 7.4; thus, the shift of fluorescence and absorption is due to binding to a site which lowers the energy of the first excited singlet state (S_1). Unlike PPIX, however, TSPP should already be in an energetically favorable conformation, since at pH 7.4 this porphyrin is water soluble due to the four SO_3^- groups.[30,58] It is also reasonable to expect that TSPP will not penetrate deeply into the tubulin interior, since the ring cannot insert into a protein site without requiring the simultaneous insertion of the large negatively charged groups. Thus, it is likely that, in order to decrease the interaction energy, the polar interactions

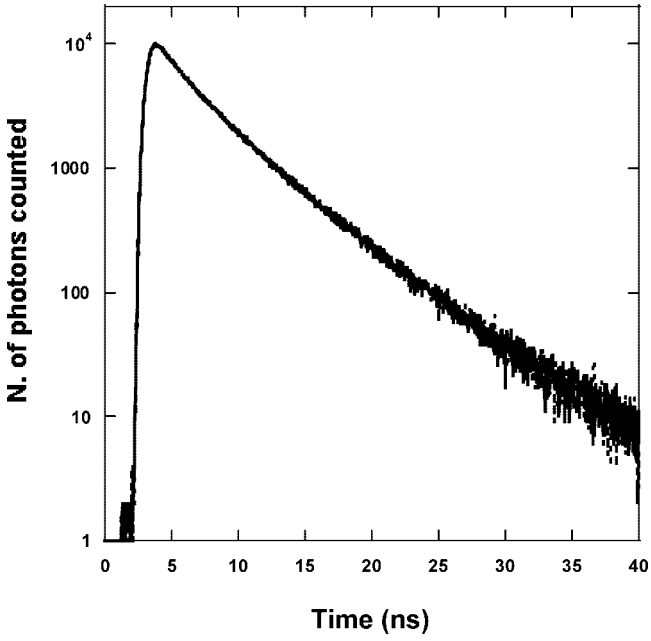

Figure 8. This figure shows the complete overlap of the tubulin decay upon addition of TSPP. The three virtually undistinguishable curves are for 1.1 μM tubulin and 0, 2.3, and 4.1 μM TSPP. Decays were recorded using pulsed excitation at 280 nm.

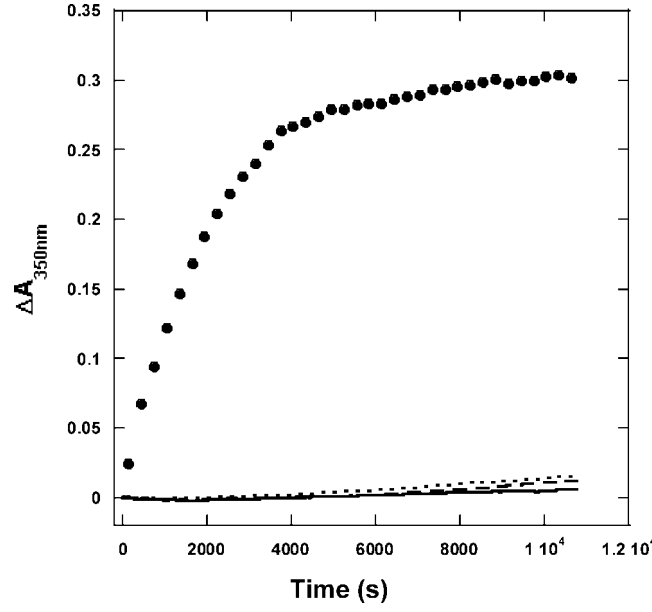

Figure 9. Polymerization of tubulin. The figure shows that under the conditions of buffer and temperature of the fluorescence experiments, 5 μM tubulin alone (—) as well as in the presence of 2.5 μM PPIX (- - -) or 2.5 μM TSPP (– – –) does not polymerize. Under the same conditions, the presence of 2.5 μM taxol (●) does instead induce polymerization.

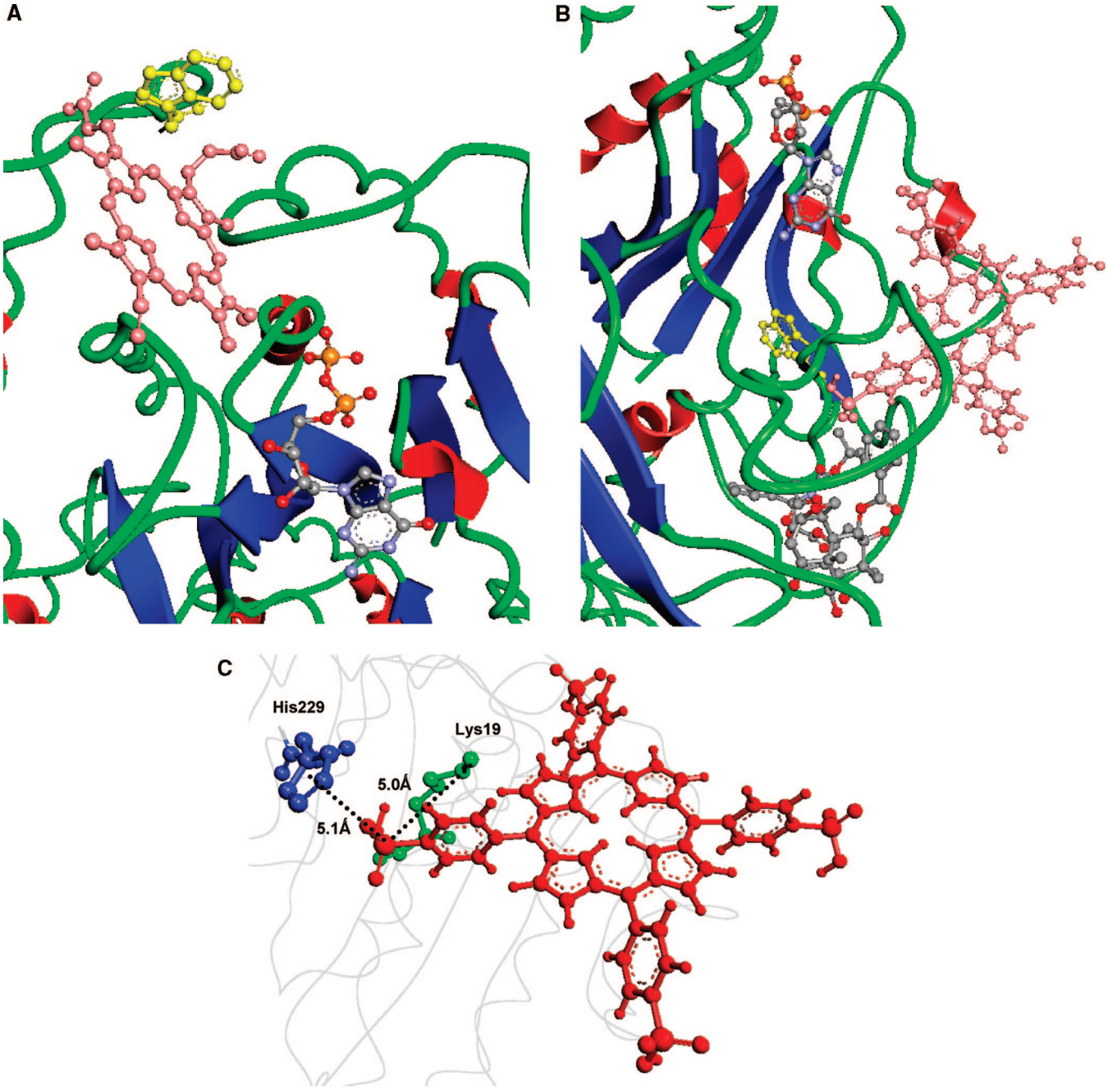

Figure 10. (A) Molecular simulations using ArgusLab show that the location of the most stable binding site for PPIX (pink) is located proximal, but not overlapped, to the nucleotide (CPK color) site and places PPIX in contact with Trp407 in the β-monomer (yellow). (B) The site of TSPP (pink) places it between the location of GTP and taxol (both in CPK colors) and at ~8 Å from Trp21 in the β-monomer (yellow). In both parts A and B, the indole ring is nearly perpendicular to the porphyrin ring. (C) One of the SO_3^- groups of TSPP (red) is in proximity and equidistant with Lys19 (green) and His229 (blue).

with the water dipoles are substituted with ionic interactions between the SO_3^- groups and basic amino acid residues. Figure 10C shows that the most energetically favorable binding site for TSPP does, indeed, locate the SO_3^- group in equidistant proximity to His229 and Lys19 where the electrostatic interaction with the charged side chains of these residues would more than compensate the loss of interaction with water molecules. The remaining three SO_3^- groups of TSPP are located at the surface of the site, thus in contact with the aqueous solvent.

The favorable energetic arrangements for PPIX and TSPP also explain the lengthening of the decay lifetime of the porphyrin fluorescence which is typical of lower energy singlet–singlet transitions.[30]

The binding constant retrieved from porphyrin fluorescence (Table 1) shows that the affinity of TSPP for the tubulin dimer is one order of magnitude larger than the one of PPIX. If the apparent dissociation constant is used to estimate the change in free energy, $\Delta G^\circ = -RT \ln(k_d)$, one obtains values of −36.2 kJ/mol for the binding of TSPP and −29.8 kJ/mol for the binding of PPIX. For TSPP, the value is in agreement with the transition from a solvated state to a stronger ionic interaction.[59–61]

The value for PPIX appears higher than expected for the transition from a "hydrated" state to the insertion (or partial insertion) into a hydrophobic pocket (typically in the order of 10 kJ/mol or less). However, the estimate could be strongly affected by the fact that PPIX forms aggregates in aqueous

solutions. Moreover, the configuration of Figure 10A shows that PPIX remains at the surface of the protein with the carboxyl tails exposed to the aqueous solvent, thus probably lowering the overall energy with a stronger interaction with the water dipoles.

The upward curvature of the Stern−Volmer plots (Figure 6) supports our interpretation of static binding. The hypothesis of partial quenching of tubulin fluorescence leads to the conclusion that TSPP quenches more Trp residues (about two per tubulin molecule) than PPIX does (a little less than one per tubulin molecule). This could be due to the fact that the size of TSPP (~2.5 nm[58] between two diametrically opposite SO_3^- groups) is approximately 40% larger than the longer side of PPIX.

Differences in the quenching rate due to quenching efficiency were ruled out by the quenching of NATA. Although the mechanism is collisional and not static, it shows that there is little difference in the quenching efficiency of the two porphyrins on Trp residues.

For both ligands, the binding constant retrieved through porphyrin fluorescence is larger than the one retrieved by quenching of tubulin. It is tempting to affirm that binding of either porphyrin may produce some conformational changes in the protein as other tubulin ligands do.[14,38,47,62–65] The blue-shift of Figure 5 is consistent with such conformational changes;[52,66,67] however, the effect is more pronounced for TSPP than PPIX. At this point of our investigation, we cannot rule either in or out porphyrin-induced conformational changes and additional studies have been currently undertaken to verify this hypothesis.

The absence of FRET suggests very close proximity between Trp residues and porphyrins. A calculation of R_0 for the Trp−porphyrin system in the complex reveals small values of 11.1 Å for PPIX and 18.2 Å for TSPP. The small value is due to the poor overlap between protein fluorescence and porphyrin absorption. Such a small value of R_0 implies that porphyrin and Trp are "nearly" in contact, thus favoring the porphyrin-induced nonradiative relaxation of the donor rather than the energy transfer to the porphyrin.[24] The docking simulations support this scenario, since they yield close contact with Trp (<5 Å with PPIX and between 8 and 10 Å with TSPP) and orthogonal orientation between the porphyrin and indole rings (both PPIX and TSPP). A likely scenario is a photoinduced electron transfer (PET) from the Trp residue(s) to the porphyrin. Assuming an oxidation potential for Trp,[68] $E_{ox}^{Trp} = 1.02$ V, and a reduction potential for the free base porphyrins,[69] $E_{red}^{PPIX} = -1.70$ V and considering the excitation energy of Trp, $E = 4.43$ eV, from the Rehm–Weller equation,[70] one can determine that the free energy for PET is a favorable $\Delta G = -1.71$ eV.

In summary, our results show that both porphyrins bind tubulin dimers with the same stoichiometry but with higher affinity for the water soluble TSPP through the formation of at least one ionic interaction. Our results also indicate that binding sites may be separate for the two porphyrins and do not seem to overlap with the sites of other known tubulin ligands. Direct evidence for this is however not available yet, since initial attempts of studying binding competition between PPIX and TSPP using optical methods were unsuccessful because of the overlap of the absorption and emission spectra of the two porphyrins. Thus, additional investigations are ongoing to establish the exact location of the binding sites and the effect of porphyrins on tubulin in vitro polymerization. This first study shows that understanding the interaction between tubulin and porphyrins may in the future offer a mechanistic explanation of the porphyrin-induced damage of microtubules and for the advancement of the use of porphyrins in phototherapy.

Acknowledgment. This work was in part funded by a Faculty Research Award of the University of Texas at San Antonio.

References and Notes

(1) Dutcher, S. K. *Curr. Opin. Cell Biol.* **2001**, *13*, 49.
(2) Amos, L. A.; Lowe, J. *Chem. Biol.* **1999**, *6*, R65.
(3) Avila, J. *FASEB J.* **1990**, *4*, 3284.
(4) Lowe, J.; Li, H.; Downing, K. H.; Nogales, E. *J. Mol. Biol.* **2001**, *313*, 1045.
(5) Bai, R.; Pei, X. F.; Boye, O.; Getahun, Z.; Grover, S.; Bekisz, J.; Nguyen, N. Y.; Brossi, A.; Hamel, E. *J. Biol. Chem.* **1996**, *271*, 12639.
(6) He, L.; Orr, G. A.; Horwitz, S. B. *Drug Discovery Today* **2001**, *6*, 1153.
(7) Richards, K. L.; Anders, K. R.; Nogales, E.; Schwartz, K.; Downing, K. H.; Botstein, D. *Mol. Biol. Cell* **2000**, *11*, 1887.
(8) Downing, K. H.; Nogales, E. *Curr. Opin. Struct. Biol.* **1998**, *8*, 785.
(9) Gabor Miklos, G. L.; Yamamoto, M. T.; Burns, R. G.; Maleszka, R. *Proc. Natl. Acad. Sci. USA* **1997**, *94*, 5189.
(10) Berg, C.; Moan, J. *Photochem. Photobiol.* **1997**, *65*, 403.
(11) Chen, Y. L.; Lin, S. Z.; Chang, J. Y.; Cheng, Y. L.; Tsai, N. M.; Chen, S. P.; Chang, W. L.; Harn, H. J. *Biochem. Pharmacol.* **2006**, *72*, 308.
(12) Rappl, C.; Barbier, P.; Bourgarel-Rey, V.; Gregoire, C.; Gilli, R.; Carre, M.; Combes, S.; Finet, J. P.; Peyrot, V. *Biochemistry* **2006**, *45*, 9210.
(13) Giannakakou, P.; Gussio, R.; Nogales, E.; Downing, K. H.; Zaharevitz, D.; Bollbuck, B.; Poy, G.; Sackett, D.; Nicolaou, K. C.; Fojo, T. *Proc. Natl. Acad. Sci.* **2000**, *97*, 2904.
(14) Geney, R.; Sun, L.; Pera, P.; Bernacki, R. J.; Xia, S.; Horwitz, S. B.; Simmerling, C. L.; Ojima, I. *Chem. Biol.* **2005**, *12*, 339.
(15) Han, Y.; Malak, H.; Chaudhary, A. G.; Chordia, M. D.; Kingston, D. G. I.; Bane, S. *Biochemistry* **1998**, *37*, 6636.
(16) Rao, S.; Orr, G. A.; Chaudahary, A. G.; Kingston, D. G. I.; Horwitz, S. B. *J. Biol. Chem.* **1995**, *270*, 20235.
(17) Madiraju, C.; Edler, M. C.; Hamel, E.; Raccor, B. S.; Balachandran, R.; Zhu, G.; Giuliano, K. A.; Vogt, A.; Shin, Y.; Fournier, J. H.; Fukui, Y.; Bruckner, A. M.; Curran, D. P.; Day, B. W. *Biochemistry* **2005**, *44*, 15053.
(18) Gigant, B.; Wang, C.; Ravelli, R. B. G.; Roussi, F.; Steinmetz, M. O.; Curmi, P. A.; Sobel, A.; Knossow, M. *Nature* **2005**, *435*, 519.
(19) Berg, K.; Moan, J. *Photochem. Photobiol.* **1992**, *56*, 333.
(20) Boekelheide, K.; Eveleth, J.; Tatum, A. H.; Winkelman, J. W. *Photochem. Photobiol.* **1987**, *46*, 657.
(21) Fotinos, N.; Campo, M. A.; Popowycz, F.; Gurny, R.; Lange, N. *Photochem. Photobiol.* **2006**, *82*, 994.
(22) Kennedy, J. C.; Marcus, S. L.; Pottier, R. H. *J. Clin. Laser Med. Surg.* **1996**, *14*, 289.
(23) Brancaleon, L.; Moseley, H. *Biophys. Chem.* **2002**, *96*, 77.
(24) Tian, F.; Johnson, K.; Lesar, A. E.; Moseley, H.; Ferguson, J.; Samuel, I. D. W.; Mazzini, A.; Brancaleon, L. *Biochim. Biophys. Acta* **2005**, *1760*, 38.
(25) Eftink, M. R.; Ghiron, C. A. *Anal. Biochem.* **1981**, *114*, 189.
(26) Eftink, M. R. *Biophys. J.* **1994**, *66*, 482.
(27) Lakowicz, J. R. *Photochem. Photobiol.* **2000**, *72*, 421.
(28) Beltramini, M.; Firey, P. A.; Ricchelli, F.; Rodgers, M. A. J.; Jori, G. *Biochemistry* **1987**, *26*, 6852.
(29) Waterman-Storer, C. M.; Salmon, E. D. *Biophys. J.* **1998**, *75*, 2059.
(30) Andrade, S. M.; Costa, S. M. B. *Biophys. J.* **2002**, *82*, 1607.
(31) Hall, D.; Minton, A. P. *Anal. Biochem.* **2005**, *345*, 198.
(32) Horowitz, P.; Prasad, V.; Luduena, R. F. *J. Biol. Chem.* **1984**, *259*, 14647.
(33) Avdulov, N. A.; Chochina, S. V.; Daragan, V. A.; Schroeder, F.; Mayo, K. H.; Wood, W. G. *Biochemistry* **1996**, *35*, 340.
(34) Bagdonas, S.; Ma, L. W.; Iani, V.; Rotomskis, R.; Juzenas, P.; Moan, J. *Photochem. Photobiol.* **2000**, *72*, 186.
(35) Cantor, C. R.; Schimmel, P. R. *Biophysical Chemistry part II: Techniques for the study of biological structure and function*; W.H. Freeman and company: New York, 1980; p 846.
(36) Davila, J.; Harriman, A. *J. Am. Chem. Soc.* **1990**, *112*, 2682.
(37) Lakowicz, J. R. *Principles of fluorescence spectroscopy*; Plenum Press: New York, 1983.
(38) Sackett, D. L. *Biochemistry* **1995**, *34*, 7010.
(39) Lakowicz, J. R. *Principles of Fluorescence Spectroscopy*; Kluwer Academic/Plenum: New York, 1999.
(40) Lehrer, S. S. *Biochemistry* **1971**, *10*, 3254.

(41) Tatikolov, A. S.; Costa, S. M. *Photochem. Photobiol.* **2004**, *80*, 250.
(42) London, E.; Feigenson, G. W. *Biochemistry* **1981**, *20*, 1932.
(43) Lehrer, S. S.; Fasman, G. D. *Biochem. Biophys. Res. Commun.* **1966**, *23*, 133.
(44) Chipman, D. M.; Grisaro, V.; Sharon, N. *J. Biol. Chem.* **1967**, *242*, 4388.
(45) Macaroff, P. P.; Oliveira, D. M.; Lacava, Z. G. M.; Azevedo, R. B.; Lima, E. C. D.; Morais, P. C.; Tedesco, A. C. *IEEE Trans. Magn.* **2004**, *40*, 3027.
(46) Stryer, L. *Annu. Rev. Biochem.* **1978**, *47*, 819.
(47) Ray, K.; Bhattacharyya, B.; Biswas, B. B. *J. Biol. Chem.* **1981**, *256*, 6241.
(48) Ricchelli, F.; Stevanin, D.; Jori, G. *Photochem. Photobiol.* **1988**, *48*, 13.
(49) Brancaleon, L.; Magennis, S. W.; Samuel, I. D. W.; Namdas, E.; Lesar, A.; Moseley, H. *Biophys. Chem.* **2004**, *109*, 351.
(50) Aveline, B. M.; Hasan, T.; Redmond, R. W. *J. Photochem. Photobiol., B* **1995**, *30*, 161.
(51) Dahms, T. E. S.; Willis, K. J.; Szabo, A. G. *J. Am. Chem. Soc.* **1995**, *117*, 2321.
(52) Samanta, U.; Pal, D.; Chakrabarti, P. *Proteins* **2000**, *38*, 288.
(53) Tanaka, F.; Kaneda, N.; Mataga, N.; Tamai, N.; Yamazaki, I.; Hayashi, K. *J. Phys. Chem.* **1987**, *91*, 6344.
(54) Ross, J. B. A.; Schmidt, C. J.; Brand, L. *Biochemistry* **1981**, *20*, 4369.
(55) Ricchelli, F.; Gobbo, S.; Moreno, G.; Salet, C.; Brancaleon, L.; Mazzini, A. *Eur. J. Biochem.* **1998**, *253*, 760.
(56) Lang, K.; Mosinger, J.; Wagnerova, D. M. *Coord. Chem. Rev.* **2004**, *248*, 321.
(57) Ricchelli, F.; Gobbo, S.; Jori, G.; Moreno, G.; Salet, C. *Eur. J. Biochem.* **1995**, *233*, 159.
(58) Kelbauskas, L.; Bagdonas, S.; Dietel, W.; Rotomskis, R. *J. Luminesc.* **2003**, *101*, 253.
(59) Raschke, T. M.; Tsai, J.; Levitt, M. *Proc. Natl. Acad. Sci.* **2001**, *98*, 5965.
(60) Rick, S. W.; Berne, B. J. *J. Phys. Chem. B* **1997**, *101*, 10488.
(61) Canadas, O.; Saenz, A.; Orellana, G.; Casals, C. *Anal. Biochem.* **2005**, *340*, 57.
(62) Howard, W. D.; Timasheff, S. N. *J. Biol. Chem.* **1988**, *263*, 1342.
(63) Kumar, N. *J. Biol. Chem.* **1981**, *256*, 10435.
(64) Uppuluri, S.; Knipling, L.; Sackett, D. L.; Wolff, J. *Proc. Natl. Acad. Sci. USA* **1993**, *90*, 11598.
(65) Sharma, S.; Ganesh, T.; Kingston, D. G.; Bane, S. *Anal. Biochem.* **2007**, *360*, 56.
(66) Harvey, B. J.; Bell, E.; Brancaleon, L. *J. Phys. Chem. B* **2007**, *111*, 2610.
(67) Sharma, V. K.; Kalonia, D. S. *J. Pharm. Sci.* **2003**, *92*, 890.
(68) DeFelippis, M. R.; Murthy, C. P.; Broitman, F.; Weinraub, D.; Faraggi, M.; Klapper, M. H. *J. Phys. Chem.* **1991**, *95*, 3416.
(69) Worthington, P.; Hambright, P.; Williams, R. F. X.; Reid, J.; Burnham, C.; Shamim, A.; Turay, J.; Bell, D. M.; Kirkland, R.; Little, R. G.; Datta-Gupta, N.; Eisner, U. *J. Inorg. Biochem.* **1980**, *12*, 281.
(70) Rehm, D.; Weller, A. *Isr. J. Chem.* **1970**, *8*, 259.

BM700687X